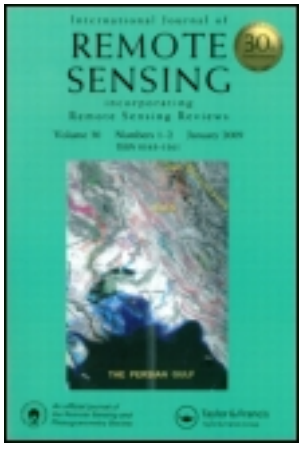

International Journal of Remote Sensing

Publication details, including instructions for authors and subscription information:
http://www.tandfonline.com/loi/tres20

Combining satellite data for estimation of rainfall for analysis of a watershed scale

Hsiao-Ping Wei [a], Keh-Chia Yeh [a], Gin-Rong Liu [b] & Chun-Chieh Chao [c]

[a] Department of Civil Engineering, National Chiao Tung University, Hsinchu, Taiwan, ROC

[b] Center for Space and Remote Sensing Research, National Central University, Tao-Yuan, Taiwan, ROC

[c] Institute of Atmospheric Physics, National Central University, Tao-Yuan, Taiwan, ROC

Published online: 08 Aug 2011.

To cite this article: Hsiao-Ping Wei, Keh-Chia Yeh, Gin-Rong Liu & Chun-Chieh Chao (2011) Combining satellite data for estimation of rainfall for analysis of a watershed scale, International Journal of Remote Sensing, 32:22, 6945-6959, DOI: 10.1080/01431161.2010.517227

To link to this article: http://dx.doi.org/10.1080/01431161.2010.517227

International Journal of Remote Sensing
Vol. 32, No. 22, 20 November 2011, 6945–6959

Taylor & Francis
Taylor & Francis Group

Combining satellite data for estimation of rainfall for analysis of a watershed scale

HSIAO-PING WEI*†, KEH-CHIA YEH†, GIN-RONG LIU‡ and CHUN-CHIEH CHAO§

†Department of Civil Engineering, National Chiao Tung University, Hsinchu, Taiwan, ROC

‡Center for Space and Remote Sensing Research, National Central University, Tao-Yuan, Taiwan, ROC

§Institute of Atmospheric Physics, National Central University, Tao-Yuan, Taiwan, ROC

(*Received 16 July 2009; in final form 8 July 2010*)

The microwave/infrared rainfall algorithm (MIRA) method combines microwave and infrared channels for their respective contributions to the achievement of higher rainfall-correlated and spatial resolution data, in order to acquire appropriate rainfall data for hydrological models. In this study, estimates of rainfall rate using the MIRA method are affected by the time lag between the data acquisition of the microwave and infrared channels. The root-mean-square error (RMSE) for comparing the rainfall rate retrieved by the MIRA method (5-minute time lag between microwave and infrared data) to the ground rainfall rate in Taiwan is 12.23 mm hour^{-1} with a correlation coefficient of 0.58. In addition, by comparing rainfall estimated by the TMI-2A12 and the MIRA method for three typhoons, the rainfall estimated by the latter method is more significantly correlated with the ground-observed rainfall.

1. Introduction

Climate change may be the most challenging issue that the world faces nowadays. In the era of climate change, much attention should be paid to extreme weather events, such as severe rainfall, extreme flood and persistent drought (IPCC 2001). Heavy rainfall caused by typhoons results in both human-life and financial loss in Taiwan every year. This is especially the cases for slow-moving typhoons, which can bring severe disasters such as large-scale floods and debris flows. Therefore, one of the most important topics in natural disaster-prevention practice in Taiwan would be the accurate prediction of typhoon rainfall distribution.

Traditionally, the estimation of rainfall for a given watershed is carried out by using ground rain gauges, ground-based radars and meteorological satellites. Data gathered by satellite could cover a large area with satisfactory spatial resolution. Therefore, increasing attention in recent years has focused on the rainfall estimation using meteorological satellites. Initially, rainfall estimation using meteorological satellite data was accomplished by visible and/or infrared images of clouds. Barrett and Martin (1981)

*Corresponding author. Email: kelly.cv92g@nctu.edu.tw

International Journal of Remote Sensing
ISSN 0143-1161 print/ISSN 1366-5901 online © 2011 Taylor & Francis
http://www.tandf.co.uk/journals
http://dx.doi.org/10.1080/01431161.2010.517227

used such images to develop three methods for the estimation of rainfall: the cloud indexing method, the threshold method and the life-span method. However, the visible channel can only be used in the daytime. Both the visible and the infrared channels measure cloud-top characteristics, which poorly correlate to the actual rainfall on the ground. Therefore, using visible and infrared images is considered an indirect estimation of rainfall. Since microwaves can penetrate cloud, the observations can be used to estimate directly the rainfall beneath the cloud. Hollinger (1989), Chiu *et al.* (1990), Adler *et al.* (1991), Hollinger (1991), Ferraro (1997) and Kidder *et al.* (2005) used microwaves for the development of rainfall-estimation equations. Although rainfall estimations using microwave data are more accurate than those using infrared, microwaves are restricted by their radiation capacity and thus have a substantially lower spatial resolution compared to infrared.

Studies by Xu *et al.* (1999), Todd *et al.* (2000), Kidd *et al.* (2003) and Huffman *et al.* (2007) combined microwave and infrared data in an attempt to improve the temporal and spatial resolution in order to increase the accuracy of rainfall estimation. Todd *et al.* (2000) adopted a rainfall rate of 0.1 mm hour^{-1} estimated by microwave as the threshold value for infrared to judge whether or not it was raining. By using infrared brightness temperature data, the rainfall rates estimated by microwave could then be adjusted. When the spatial resolution was 110 km, the estimated rainfall by combining microwave and infrared data was compared with that observed from the EPSAT network of rain gauges under the HAPEX-SAHEL project. The root-mean-square error (RMSE) was 2.04 mm day^{-1} with a correlation coefficient of 0.96. Kidd *et al.* (2003) developed a combined infrared and microwave rainfall estimation technique, that is, a cumulative histogram matching approach, to generate an infrared temperature–microwave rainfall rate relationship. When the spatial resolution was 12 km, the estimated rainfall data compared with those obtained from the ground rain gauges had a RMSE of 10 mm month^{-1}, with a Pearson's correlation coefficient of 0.3. Huffman *et al.* (2007) combined multiple passive microwave estimates and microwave-calibrated infrared (IR) estimates. They derived linear relationships between surface precipitation accumulation and IR brightness temperatures. When the spatial resolution was 55 km, the estimated rainfall data compared with those obtained from the validation data had a correlation coefficient of 0.9. In the methods mentioned above, microwave data are used to calibrate the infrared parameters in order to increase the temporal resolution. However, this article proposes a method whereby the Special Sensor Microwave Image (SSM/I) and infrared (IR1) data are combined in order to increase the spatial resolution of SSM/I data without the loss of rainfall estimated from the microwave data.

The major watershed areas in Taiwan range from 300 to 3000 km^2. The spatial resolution for the rainfall data gathered by the microwave channels is usually too coarse for the hydrological models. In view of this and the different characteristics of the visible, infrared and microwave channels, this study utilizes the satellites Geostationary Meteorological Satellite 5 (GMS-5), Geostationary Operational Environmental Satellite 9 (GOES-9) and Multi-functional Transport Satellite-1R (MTSAT-1R) brightness temperature (infrared) data to redistribute the rainfall distribution in the field of view (FOV) by microwave (SSM/I). It is expected that the spatial resolution of rainfall estimated by microwave (25 km) could be improved by combining it with the infrared information (with a resolution of 5 km). This method is known as the microwave/infrared rainfall algorithm (MIRA) in this study. The term

MIRA was also used by Todd *et al.* (2000). Since the ground rain-gauge data are usually assumed as the true values, this study uses ground rain-gauge data to evaluate the accuracy of the estimated rainfall rate obtained by the MIRA method, as well as the estimated rainfall rate inversed from the Tropical Rainfall Measuring Mission (TRMM) microwave (TMI-2A12, TMI-3B42) data provided by NASA.

Attributed to global warming, more and more extreme rainfall events have occurred recently all over the world. This has increased the need for better observations and predictions for such events. In addition to rain-gauge and radar data, satellite data could also be used to record extreme rainfall, and this could be more efficient than other methods because of its broader scanning coverage. Currently, the spatial resolution of retrieved rainfall using SSM/I data is about 25 km, which is too coarse to capture the detail of an extreme rainfall event. In this study, SSM/I data blended with infrared data are used to improve the spatial resolution and to monitor extreme rainfall.

2. Data set description

This study utilizes the data gathered from microwave and infrared channels of various satellites, and the ground rain gauges. These data are described below.

2.1 *Microwave and infrared data*

The data collected by the microwave channels are provided by the SSM/I under the U.S. Defense Meteorological Satellites Program (DMSP) and the Microwave Imager (TMI) under the TRMM. The IR1 brightness temperature data are obtained from the GMS-5, the GOES-9 and the MTSAT-1R.

The SSM/I are seven-channel passive microwave radiometers scanning in the dual-polarized (vertical and horizontal) channels at 19.35, 37.0 and 85.5 GHz, and vertical-polarized channels at 22.2 GHz (Hollinger 1989). The SSM/I scans can be categorized into the A-Scan and the B-Scan. For the A-scan, the spatial resolution is 25 km at 19.35, 22.2 and 37.0 GHz. The B-scan, on the other hand, only has an observed value at 85 GHz with a spatial resolution of 12.5 km. The TRMM Microwave Imager (TMI) is modified from the SSM/I with two main differences: the addition of a pair of 10.7 GHz channels with horizontal and vertical polarizations; and the frequency of the water-vapour channel being changed from 22.2 to 21.3 GHz. Therefore, the TMI has nine-channel passive microwave radiometers at five frequencies (10.7, 19.4, 21.3, 37.0 and 85.5 GHz) with dual-polarization (except at 21.3 GHz, which is vertical-polarized only). The effective ground resolution of the TMI data varies from 9.1 to 4.6 km (Kummerow 1998).

The GMS-5 satellite was operated by the Japan Meteorological Agency (JMA), launched in 1995. When its service lifetime ended on 22 May 2003, GMS-5 was temporarily replaced by the United States' NOAA GOES-9 satellite, until MTSAT-1R was back to its normal operation in February 2005. The GMS-5 satellite had four channels: one visible (VIS: 0.55–0.75 μm), two infrared (IR1: 10.5–11.5 μm; IR2: 11.50–12.50 μm) and one water vapour (WV: 6.50–7.00 μm). The visible and infrared channels of GMS-5 had spatial resolutions of 1.25 and 5 km respectively. GOES-9 is similar to GMS-5. It has one visible channel (VIS: 0.55–0.75 μm), two infrared channels (IR1: 10.20–11.20 μm; IR2: 11.50–12.50 μm) and one water-vapour channel (WV: 6.50–7.00 μm). As well as the visible (VIS: 0.55–0.8 μm) channel, two infrared channels (IR1: 10.30–11.30 μm; IR2: 11.50–12.50 μm) and one water-vapour channel (WV: 6.50–7.00 μm), MTSAT-1R has one additional near infrared channel (near IR:

3.5–4.0 μm). The IR1 spatial resolution for the infrared channels of the GOES-9 and MTSAT-1R satellites are 1 and 4 km respectively.

This study utilizes the microwave data from 2000 to 2005 observed by SSM/I, TMI-2A12 and TMI-3B42. The SSM/I data are adopted from the DMSP F-13, F-14 and F-15 satellites. The associated rain information obtained from the TMI-2A12 data includes cloud liquid water, precipitation water and latent heat. The TMI-3B42 data uses the TMI-2A12 rain estimates to obtain high temporal resolution (three-hourly) IR rain rates over daily gridded 27.5 km × 27.5 km boxes (Huffman *et al.* 1995, Huffman *et al.* 2007). The infrared data are taken from GMS-5 from August 2000 to April 2003. The data from April 2003 to December 2004 are observed by GOES-9, while MTSAT-1R is responsible for data in 2005. The GMS-5, GOES-9 and MTSAT-1R data from IR1 are used for brightness temperature. In order to ensure the consistency of the infrared data, all data are remapped to an approximate 5-km pixel resolution by the nearest neighbourhood method (Sonka *et al.* 1999).

2.2 *Typhoon and ground rain-gauge data*

The redistribution of rainfall rates estimated by microwave (SSM/I) and infrared IR1 (GMS-5, GOES-9 and MTSAT-1R) were compared and verified with the hourly rainfall data gathered at 372 gauge stations in Taiwan, as shown in figure 1. The hourly rainfall data from 2000 to 2005 were downloaded from the research data base of the Department of Atmospheric Sciences, National Taiwan University (http://dbar.as.ntu.edu.tw/). This study collected 17 typhoon events during the above-mentioned time periods, as shown in table 1.

3. The MIRA method

When applying the satellite rainfall data to the watershed rainfall-runoff modelling, it is necessary to consider the level of resolution. Turk *et al.* (2000) pointed out that the estimated rainfall amount using satellite data was affected by the temporal and spatial resolutions. The correlation coefficient between the rain-gauge observed rainfall and the estimated rainfall based on 110 km spatial resolution (daily) was about 0.65, and about 0.15 for that based on 11 km spatial resolution (hourly). Wei (2003) proposed a reasonable spatial resolution of 5 km × 5 km grid for the estimation of rainfall in Taiwan. Therefore, all the infrared data are remapped to an approximate 5-km pixel resolution in this study.

In this study, we combine the microwave and infrared channels for their respective contributions to the achievement of higher rainfall-correlated and higher spatial resolution data, in order to acquire appropriate rainfall data for hydrological models. The procedure for the combination of microwave (SSM/I) and infrared (IR1) data in this study consists of three steps. The first step is the retrieval of the rainfall rate ($R_{\mathrm{SSM/I}}$) from the microwave data (SSM/I). The second step is the identification of rain areas from the FOV of SSM/I data using co-existing IR1 pixels. The third step is the combination of the infrared and microwave data obtained from the above two steps, and the redistribution of the estimated rainfall ($R_{\mathrm{SSM/I}}$) using the infrared (IR1) brightness temperature data in rain areas. The flow chart for the combination of SSM/I and IR1 data is shown in figure 2. The three steps are described below.

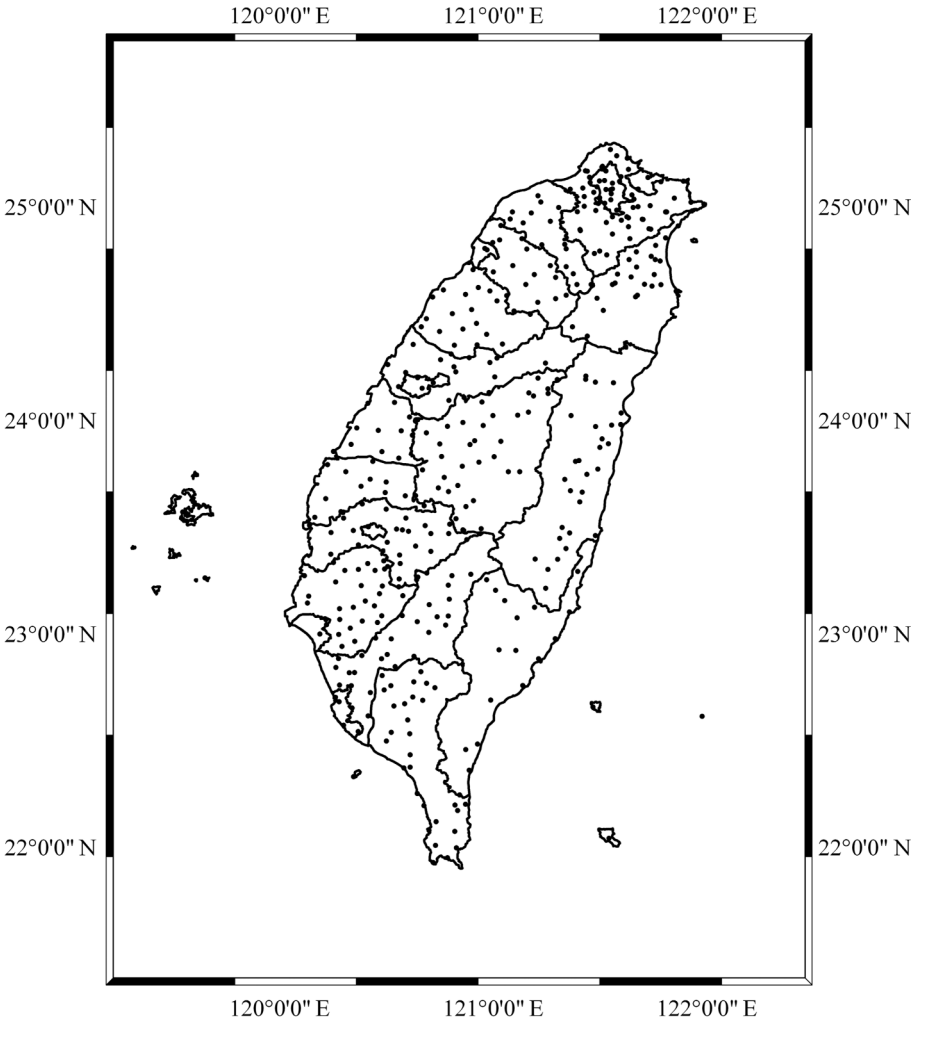

Figure 1. Ground rain gauges in Taiwan.

Table 1. Typhoon data collected in this study.

Year	Typhoon
2000	Bilis, Prapiroon, Xangsane
2001	Trami, Toraji, Nari, Lekima
2002	Nakri
2003	Morakot, Dujuan, Melor
2004	Aere, Haima, Nock-Ten, Nanmadol
2005	Haitang, Damrey

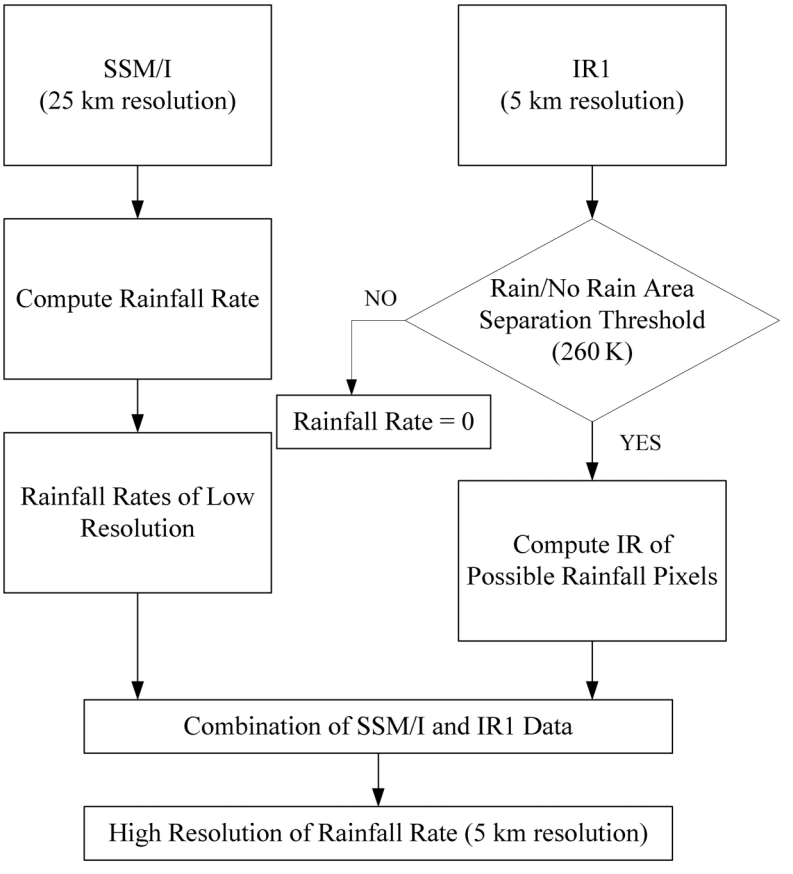

Figure 2. Flow chart for the combination of microwave and infrared data.

3.1 *Estimation of rainfall rate by microwave data*

Ho (2005) used the rainfall formulae developed by Chiu *et al.* (1990) and Ferraro (1997) and retrieved the rainfall rates of the 34 typhoons that passed through the coastal zones of Taiwan from 2000 to 2004. The R^2 (coefficient of determination) values for the retrieved rainfall rate are 0.66 and 0.72 for Chiu *et al.* and Ferraro respectively. Therefore, this study utilizes the rainfall formula developed by Ferraro (1997) to retrieve the rainfall rate ($R_{\mathrm{SSM/I}}$) from the typhoons passing through Taiwan from 2000 to 2005. The equations are shown below:

Inland:

$$\mathrm{SI_L} = [451.9 - 0.44T_{b\_19v} - 1.7775T_{\mathrm{b\_22v}} + 0.00575(T_{\mathrm{b\_22v}})^2] - T_{\mathrm{b\_85v}} \quad (1)$$

$$R_{\mathrm{SSM/I}} = 0.00513[(\mathrm{SI})_{\mathrm{L}}]^{1.9468} \quad (2)$$

Ocean:

$$\mathrm{SI_W} = [-174.4 + 0.72T_{\mathrm{b\_19v}} + 2.439T_{b\_22v} - 0.00504(T_{\mathrm{b\_22v}})^2] - T_{\mathrm{b\_85v}} \quad (3)$$

$$R_{\mathrm{SSM/I}} = 0.00188[(\mathrm{SI})_{\mathrm{w}}]^{2.0343} \tag{4}$$

where $\mathrm{SI_L}$ and $\mathrm{SI_w}$ represent the inland and ocean scattering indices respectively; $T_{\mathrm{b\_19v}}$, $T_{\mathrm{b\_22v}}$ and $T_{\mathrm{b\_85v}}$, represent the brightness temperatures of vertical-polarized channels at 19.35, 22.0 and 85.5 GHz respectively (the unit of the brightness temperature is the absolute temperature in Kelvin); and $R_{\mathrm{SSM/I}}$ represents the retrieved rainfall rate (mm hour^{-1}).

3.2 *Identification of rain areas using infrared data*

Usually the identification of rain areas is conducted prior to the estimation of rainfall using the satellite's data. Currently, many researchers use infrared data to identify the rain areas. Arkin and Meisner (1987) and Barrett and Beaumont (1994) conducted an estimation of convective rainfall and therefore chose a lower infrared threshold that ranged from 220 K to 235 K. Todd *et al.* (2000) indicated an IR threshold varying with time and space. For the tropical and the humid mid-latitude regions, thresholds are between 260 K and 290 K. This study adopts the infrared (IR1) threshold of 260 K proposed by Todd *et al.* (2000) for the identification of rain areas.

3.3 *Combination of infrared and microwave data*

The emissive energy from the microwave channel is weaker than that from the infrared, which needs a larger scan area for the microwave to receive sufficient energy and, as a result, has a lower spatial resolution compared to infrared. On the other hand, the estimated rainfall from the cloud-top data collected by infrared is less correlative to the real rainfall observed by the gauge station. Therefore, this study redistributes the retrieved rainfall rate ($R_{\mathrm{SSM/I}}$) estimated by Ferraro's (1997) formula in the SSM/I FOV by using the cloud-top brightness temperature measured by the infrared (IR1). Four scenarios for this combined method of the microwave (SSM/I) and the infrared (IR1) data are shown in table 2. Two of the four scenarios have rainfall, which can be estimated as follows.

(1) *Rainfall rate estimated by both microwave and infrared data*. When the rainfall rate ($R_{\mathrm{SSM/I}}$) retrieved from the microwave data (25-km resolution) FOV is not 0 within the rain area identified by the infrared data (5-km resolution), the redistribution of rainfall rate by the infrared brightness temperature is:

$$R_i = R_{\mathrm{SSM/I}} \frac{\Delta T_i}{\sum_{i=1}^{\mathrm{total}\leq 25} \Delta T_i} \tag{5}$$

Table 2. Four scenarios for the combining of the microwave (SSM/I) and infrared (IR1) data.

		Microwave (SSM/I)	
		Rain area	No rain area
Infrared (IR1)	Rain area	Equation (5)	No rainfall
	No rain area	Equation (6)	No rainfall

where R_i (mm hour^{-1}) is the redistributed rainfall rate for the finer cell i by combining the SSM/I and the IR1 brightness temperature data; total is the number of infrared (IR1) FOV in a SSM/I FOV; $R_{\mathrm{SSM/I}}$ is the rainfall rate in a SSM/I FOV found by inverting equations (3) and (4); ΔT_i is the temperature difference between the infrared brightness temperature and the threshold value (260 K); and $\sum_{i=1}^{total \leq 25} \Delta T_i$ is the summation of all ΔT_i in a given SSM/I FOV.

(2) *Rainfall rate estimated by microwave data*. When the retrieved rainfall rate ($R_{\mathrm{SSM/I}}$) from the microwave data FOV is not 0 within the no rain area identified by the infrared data, the rainfall rate in the FOV of the microwave (SSM/I) channel can be estimated by:

$$R_i = R_{\mathrm{SSM/I}} \tag{6}$$

4. Case study

Seventeen typhoons occurring during 2000–2005 in Taiwan were selected, and they were scanned by the microwave and infrared satellites, with the scanning time lags between the satellites being within 1 hour. Fifty-seven sets of satellite data were in compliance with the above-mentioned conditions. Among the 17 typhoons, Bilis (in 2000) and Haitang (in 2005) are classified as the strongest typhoons. According to the report from the Central Weather Bureau, Taiwan, typhoon Bilis resulted in 11 fatalities, 4 missing people, 434 destroyed houses and economic damage amounting to nearly 4.7 billion NT dollars. Typhoon Haitang resulted in 12 fatalities, 3 missing people and economic damage amounting to nearly 4.8 billion NT dollars.

The results of two rainfall-rate estimations using the MIRA method for typhoons Bilis (in 2000) and Haitang (in 2005) at specified time periods are shown in figures 3 and 4. Figure 3(*a*) shows the retrieved rainfall rate of typhoon Bilis using equations (3) and (4), with the SSM/I data observed at 00:18 UTC on 23 August 2000. In figure 3(*b*), the GMS-5 infrared satellite data were observed at 00:00 UTC on 23 August 2000. The rainfall rate in figure 3(*c*) is a combination of the estimated rainfall in figure 3(*a*) and (*b*) using the MIRA method. Figure 3(*d*) shows the comparison of different rainfall-rate estimations for a local plain located in the central region of Taiwan. Figure 4(*a*) reveals the retrieved rainfall rate of typhoon Haitang using equations (3) and (4), with the SSM/I data observed at 01:59 UTC on 18 July 2005. In figure 4(*b*), the MTSAT-1R infrared satellite image data were observed at 02:00 UTC on 18 July 2005. Figure 4(*c*) shows the redistributed rainfall according to the data in figure 4(*a*) and (*b*) by using the MIRA method. Figure 4(*d*) shows the comparison of different rainfall-rate estimations for a local mountain area located in the central region of Taiwan. The rainfall rate distributions using SSM/I and MIRA data are expressed in a shaded colour for easier recognition. Higher rainfall rates are marked in a darker red colour. Since lower brightness temperature might cause larger rainfall, lower brightness temperature values are marked in a darker red colour.

From figures 3 and 4, it can be seen that the distribution pattern of the rainfall rate by using the MIRA method is different from the original pattern estimated by the SSM/I data. It can be seen from figure 3(*d*) that the rainfall rate decreases from the south-west corner towards the north corner of the local area according to the rainfall rate observed by rain gauges, which can be reasonably estimated by the MIRA method using the brightness temperature infrared data to adjust the rainfall rate retrieved by

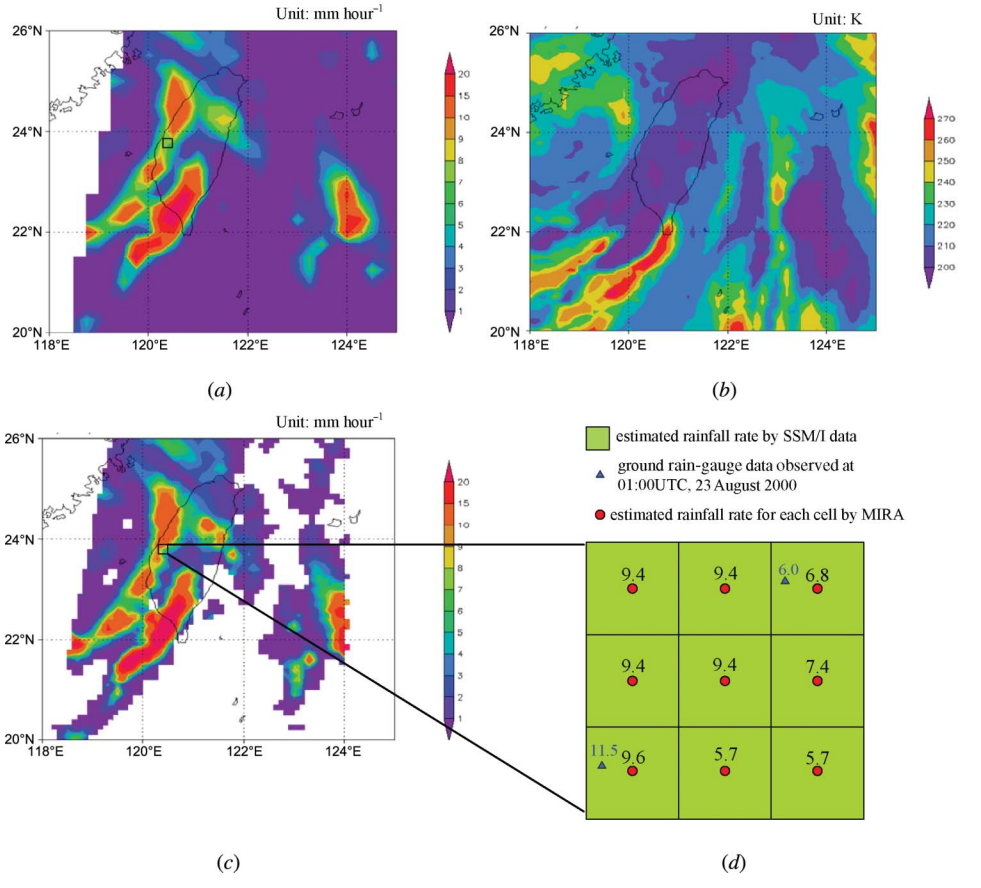

Figure 3. (*a*) Inversed rainfall rate of typhoon Bilis using equations (3) and (4), with the microwave (SSM/I) data observed at 00:18 UTC on 23 August 2000; (*b*) GMS-5 infrared satellite images (IR1) observed at 00:00 UTC on 23 August 2000; (*c*) estimated rainfall using the MIRA method by combining the data in (*a*) and (*b*); and (*d*) rainfall-rate estimations for a local area.

the SSM/I data. Similarly, as can be seen from figure 4(*d*), the tendency of the rainfall rate increases from the south-west towards the north of the local mountain area, which can also be well estimated by the proposed MIRA method.

5. Verification and discussion of the results

The statistical measures used to compare the satellite estimates of rainfall rates (MIRA method, microwave SSM/I, TMI-2A12 and TMI-3B42) with measurements from ground rain gauges are the RMSE and the correlation coefficient (CC).

5.1 *Results of verification between the MIRA and the ground rainfall data*

The MIRA method developed in this study estimates the spatial rainfall data and compares them with data gathered at the nearest ground rain-gauge stations. In addition, it takes time for a raindrop falling from the cloud to reach the ground. Hence, the time

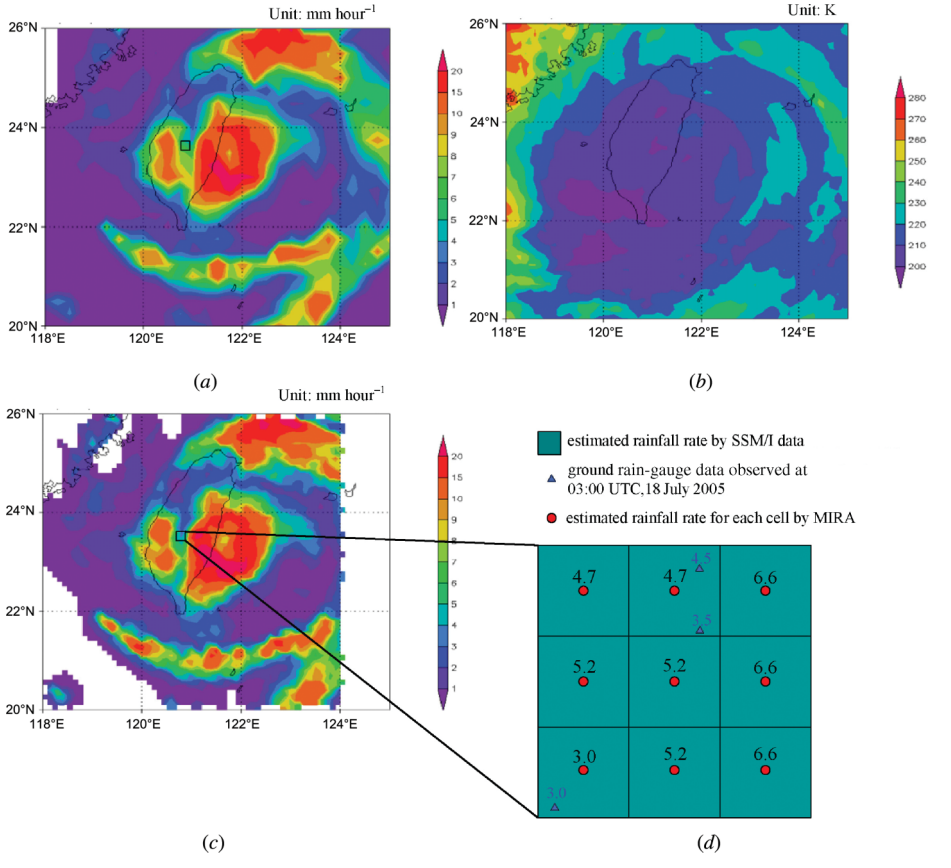

Figure 4. (*a*) Inversed rainfall rate of typhoon Haitang using equations (3) and (4), with the microwave (SSM/I) data observed at 01:59 UTC on 18 July 2005; (*b*) MTSAT-1R infrared satellite image (IR1) observed at 02:00 UTC on 18 July 2005; (*c*) estimated rainfall using the MIRA method by combining the data in (*a*) and (*b*); and (*d*) rainfall-rate estimations for a local area.

lag of collection between the SSM/I data and rain-gauge data needs to be considered. Determination of time lag is based on finding the largest correlation coefficient between the two data sets, that is SSM/I data and rain-gauge data. In this article, typhoons Bilis (in 2000), Prapiroon (in 2000) and Xangsane (in 2000) are adopted as the three cases for comparison of correlation coefficients with different collection time lags between the SSM/I data and the rainfall data gathered by the ground rain gauges.

The results are shown in table 3, from which the correlation coefficient between the rainfall rates estimated by the MIRA method and the ground rain-gauge data with a 1-hour lag is the highest. Note that the collection time lag between the IR1 and SSM/I data is 30 minutes. Therefore, we apply the ground rain-gauge data that is 1 hour later than the microwave (SSM/I) data to evaluate the accuracy of estimated rainfall rates by using the MIRA method. A total of 1736 instances of observed data were selected that complied with the above-mentioned condition. The RMSE and the correlation coefficient between the rainfall data estimated by the MIRA method and the ground rain-gauge data are 10.68 mm hour^{-1} and 0.47 respectively.

Table 3. Correlation coefficients between SSM/I data and rain-gauge data collection based on different time lags.

Typhoon	Microwave (SSM/I) image data date and time	Time lag		
		1-hour	(1-hour + 2-hour)/2	2-hour
Bilis	23 August 2000 at 00:18 UTC	0.65	0.23	0.17
Prapiroon	27 August 2000 at 11:53 UTC	0.51	0.35	0.21
Toraji	30 July 2001 at 01:08 UTC	0.66	0.51	0.22

Table 4. Comparison of results for different data-collection times for SSM/I and IR1.

Time (min)	No. of data	Correlation coefficient	RMSE (mm hour^{-1})
5	218	0.58	12.23
10	508	0.50	11.91
20	1061	0.50	11.52
25	1464	0.48	10.7

In this study, the time lags for the microwave (SSM/I) data and the infrared (IR1) data from the MIRA method were also evaluated. Four different time lags, that is, 5, 10, 20 and 25 minutes, between the microwave (SSM/I) and infrared (IR1) data were adopted. The 1-hour lag ground rain-gauge's data were used for verification. The comparison of the results for different data-collecting times from the satellites are shown in table 4. It can be seen that the RMSE and the correlation coefficient in the case of a 5-minute-lag satellite data are 12.23 mm hour^{-1} and 0.58 respectively, which is the most accurate case. According to above analysis, consideration of the collection time lag between the SSM/I and IR1 data is required and hence can increase the rainfall-rate estimation accuracy of the MIRA method.

5.2 *Results of verification of the ground rain-gauge data, the MIRA method, the microwave (SSM/I) data retrieved rainfall rate, the TMI-2A12 rainfall data and the TMI-3B42 rainfall data*

From the results mentioned above, the accuracy of the MIRA method depends on the collection time lag between the SSM/I and IR1 data. The data-collecting times for the satellites and the ground rain gauges are listed in table 5. As part of the verification, the ground rain-gauge rainfall data are compared to the MIRA rainfall rate, the microwave (SSM/I) data retrieved rainfall rate, the TMI-2A12 rainfall data and the TMI-3B42 rainfall data. The results of this comparison are shown in table 6, from which the RMSE value and the correlation coefficient between the MIRA rainfall rate and the ground rainfall rate are 13.4 mm hour^{-1} and 0.59 respectively; the RMSE value and the correlation coefficient between the TMI-2A12 rainfall rate and the ground rainfall rate are 12.7 mm hour^{-1} and 0.54 respectively; the RMSE value and the correlation coefficient between the SSM/I rainfall and the ground rainfall rate are 20.1 mm hour^{-1} and 0.67 respectively; the RMSE value and the correlation coefficient between the TMI-3B42 rainfall rate and the ground rainfall rate are 2.83 mm hour^{-1}

Table 5. Data-collection times for satellites and ground rain gauges.

No.	Typhoon	Microwave (SSM/I)	Infrared (IR1)	TMI (2A12)	TMI (3B42)	Ground rain gauge
1	Toraji	30 July 2001 at 00:44 UTC	30 July 2001 at 01:00 UTC	30 July 2001 at 00:50 UTC	30 July 2001 at 00:00 UTC	30 July 2001 at 01:00 UTC
2	Aere	24 August 2004 at 08:36 UTC	24 August 2004 at 09:00 UTC	24 August 2004 at 08:26 UTC	24 August 2004 at 09:00 UTC	24 August 2004 at 09:00 UTC
3	Haitang	17 July 2005 at 10:40 UTC	17 July 2005 at 11:00 UTC	17 July 2005 at 10:30 UTC	17 July 2005 at 09:00 UTC	17 July 2005 at 11:00 UTC

Table 6. Statistics for MIRA, TMI-2A12, SSM/I and TMI-3B42 estimates of rainfall compared with ground rain-gauge data.

Data set compared to gauge	Correlation coefficient	RMSE (mm hour^{-1})	No. of data
MIRA	0.59	13.4	86
TMI-2A12	0.54	12.7	68
SSM/I	0.67	20.1	19
TMI-3B42	0.69	2.83	11

and 0.69 respectively. Note from table 6 that the RMSE values estimated by the MIRA rainfall rate, the TMI-2A12 rainfall rate and TMI-3B42 rainfall rate are lower than that of the SSM/I rainfall rate. In addition, it can be seen that the MIRA rainfall rate has a higher correlation with the ground-observed rainfall rate than that for the TMI-2A12 rainfall data. The MIRA method can therefore improve the spatial resolution of the estimated rainfall rate and has a similar accuracy compared with the estimated rainfall rate using TMI-2A12 data with high spatial resolution. TMI-3B42 rainfall rate has a higher correlation with the ground-observed rainfall rate.

6. Conclusion and recommendation

This study proposes the method of combining microwave (SSM/I) and infrared (IR1) data for increasing the spatial resolution of SSM/I data in order to improve the accuracy of rainfall estimation for the hydrological analysis of a watershed scale in Taiwan. The data are taken from the typhoons passing through Taiwan from 2000 to 2005. By statistical comparison of the estimated rainfall rates with the rain gauges' observed data, as shown in table 6, using the data collected during three typhoon periods, the MIRA method yields satisfactory accuracy of rainfall estimation.

Since the proposed MIRA method utilizes the SSM/I data and the rainfall rate retrieved by Ferraro's (1997) equation and then redistributes them using brightness temperature data for the infrared (IR1) channels, the use of different rainfall retrieval equations would significantly affect the accuracy of the MIRA method. From the review of past research, the value of 260 K was chosen as the threshold value for the infrared (IR1) data. Since every typhoon has its own special characteristics, the use of a single threshold value to identify rain areas would result in inaccuracy. Therefore, it

is suggested that threshold values should be assigned to different types of typhoons to increase the accuracy of the MIRA method.

It can be observed from the analysis of results for typhoons Bilis (in 2000) and Haitang (in 2005) that, with the addition of infrared (IR1) brightness temperature, the MIRA method is indeed more accurate in the estimation of rain areas and more capable in contrasting and marking out the regions with intensive rainfall, which cannot be obtained using SSM/I data with coarse spatial resolution.

The use of microwave (SSM/I) data to retrieve the rainfall is affected by the time taken for the rain to reach the ground, which is influenced by atmospheric conditions (e.g. wind velocity, air drag force). Therefore, this study compares the rainfall estimated by the microwave data to the ground rain-gauge data with time lags of 1 hour, an average of 1 and 2 hours and 2 hours. It is concluded from the results that the correlation coefficient between the microwave-estimated rainfall and the ground rain-gauge data with a 1-hour lag is higher than the correlation coefficients with other time lags.

The unmatched locations and timings of the scanning of the (SSM/I) and infrared (IR1) satellites could lead to some errors. From table 4, it can be seen that when the MIRA method is used, the correlation coefficient between the (SSM/I) and infrared (IR1) data decreases when the time lag increases. It could be deduced from the current research results that the accuracy of the MIRA method is also influenced by the collection time lags for the (SSM/I) and infrared (IR1) data.

When estimating large rainfall events, the average inversed SSM/I values in the FOV would be lower than the actual rainfall. As shown in figure 5, the estimated larger rainfall values are smaller than 40 mm hour^{-1}. The improvement on this deficiency – the underestimation of rainfall at large rainfall events – should be studied in the future. Since little data gathered by the TMI satellite in this study met the desired condition of

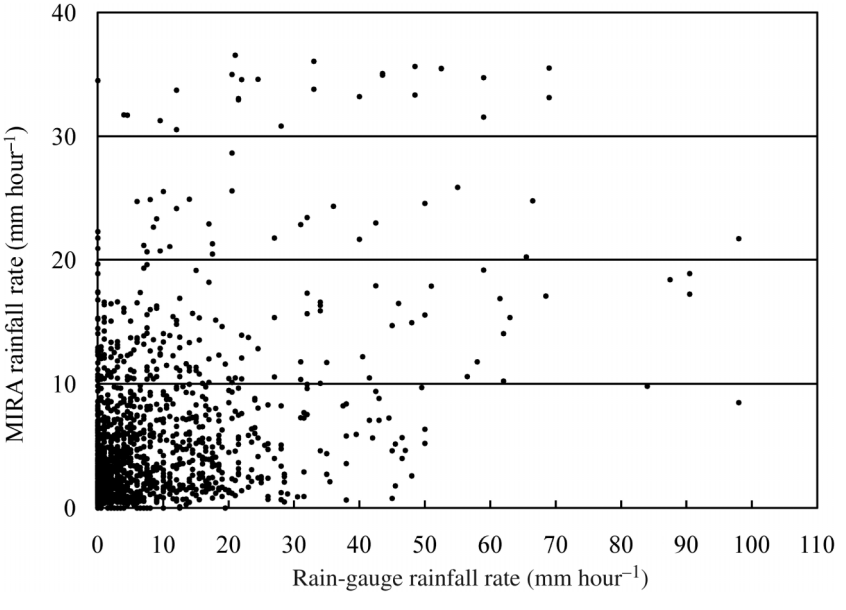

Figure 5. Comparison between the MIRA rainfall estimations and the ground rain-gauges' data (all data).

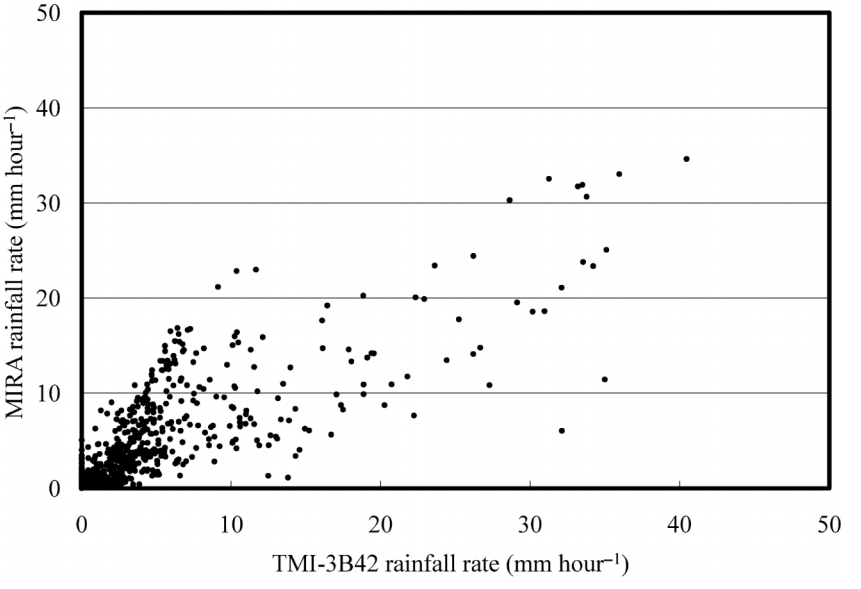

Figure 6. Comparison between the MIRA rainfall estimations and the TMI-3B42 data.

a time lag of 10 minutes or less between the TMI and SSM/I satellites, the increase of the amount of TMI data gathered in the future could further prove the soundness of the MIRA method.

From table 6, it can be seen that the correlation coefficient of TMI-3B42 is higher than that of the MIRA, but the spatial resolution of TMI-3B42 is lower than that of the MIRA. From figure 6, it is interesting to note that the correlation of rain rate estimated by the MIRA method and the TMI-3B42 data is high ($r = 0.81$). The comparison between the MIRA and the TMI-3B42 data showed good agreement.

Extreme precipitation events can cause severe damage, including loss of lives. In order to facilitate early detection of these harmful episodes, adequate spatial and temporal satellite databases must be ensured, particularly when there are fewer or no rain gauges available. The results of this study show the potential to improve spatial resolution. The addition of other microwave data (e.g. AMSU and AMSR) in the future could further improve the temporal resolution of the MIRA method. This will improve the temporal resolution and provide additional opportunity to monitor extreme rainfall events attributed to global warming. Through the intense observations of extreme rainfall events, we could obtain a better understanding of what is causing the extreme rainfall, and supply an accurate forecast for those events thereby minimizing the cost of disasters due to global warming.

References

Adler, R.F., Yeh, H.-Y.M., Prasad, N., Tao, W.K. and Simpaon, J., 1991, Microwave simulations of a tropical rainfall system with a three-dimension cloud model. *Journal of Applied Meteorology*, **30**, pp. 924–953.

Arkin, P.A. and Meisner, B.N., 1987, The relationship between large-scale convective rainfall and cold cloud over the western hemisphere during 1982–84. *Monthly Weather Review*, **115**, pp. 51–74.

Barrett, E.C. and Beaumont, M.J., 1994, Satellite rainfall monitoring: an overview. *Remote Sensing Review*, **11**, pp. 23–48.

Barrett, E.C. and Martin, D.W., 1981, *The Use of Satellite Data in Rainfall Monitoring* (London: Academic Press).

Chiu, L.S., North, G.R., Short, D.A. and Mcconnell, A., 1990, Rain estimation from satellites effect of finite field of view. *Journal of Geophysical Research*, **95**, pp. 2177–2185.

Ferraro, R.R., 1997, SSM/I derived global rainfall estimates for climatological applications. *Journal of Geophysical Research*, **102**, pp. 16 715–16 735.

Ho, T.Y., 2005, Applying SSM/I satellite data to estimate the typhoon rainfall. Master's thesis, University of Central, Taiwan.

Hollinger, J.P., 1989, DMSP Special Sensor Microwave/Imager Calibration/Validation. Space Sensing Branch, Naval Research Laboratory, Washington DC, Final report, Vol. I.

Hollinger, J.P., 1991, DMSP Special Sensor Microwave/Imager Calibration/Validation. Space Sensing Branch, Naval Research Laboratory, Washington DC, Final report, Vol. II.

Huffman, G.J., Adler, R.F., Bolvin, D.T., Gu, G., Nelkin, E.J., Bowman, K.P., Hong, Y., Stocker, E.F. and Wolff, D.B., 2007, The TRMM multi-satellite precipitation analysis: quasi-global, multi-year, combined-sensor precipitation estimates at fine scale. *Journal of Hydrometeorology*, **8**, pp. 38–55.

Huffman, G.J., Adler, R.F., Rudolph, B., Schneider, U. and Keehn, P., 1995, Global precipitation estimates based on a technique for combining satellite-based estimates, rain gauge analysis, and NWP model precipitation information. *Journal of Climate*, **8**, pp. 1284–1295.

IPCC, 2001, Climate change 2001: the scientific basis. WMO/UNEP intergovernmental panel on climate change, Third Assessment Report, Vol. I.

Kidd, C., Kniveton, D.R., Todd, M.C. and Bellerby, T.J., 2003, Satellite rainfall estimation using combined passive microwave and infrared algorithms. *Journal of Hydrometeorology*, **4**, pp. 1088–1104.

Kidder, S.Q., Kusselson, S.J., Knaff, J.A., Ferraro, R.R., Kuligowski, R.J. and Turk, M., 2005, The tropical rainfall potential (TRaP) technique, part I: description and examples. *Weather and Forecasting*, **20**, pp. 456–464.

Kummerow, C., 1998, Beamfilling errors in passive microwave rainfall retrievals. *Journal of Applied Meteorology*, **37**, pp. 356–370.

Sonka, M., Hlavac, V. and Boyle, R., 1999, *Image Processing, Analysis, and Machine Vision*, pp. 67–68 (Boston: PWS Publishing).

Todd, M.C., Kidd, C., Kniveton, D. and Bellerby, T.J., 2000, A combined satellite infrared and passive microwave technique for estimation of small-scale rainfall. *Journal of Atmospheric and Oceanic Technology*, **18**, pp. 742–755.

Turk, F.J., Hawkins, J., Smith, E.A., Marzano, F.S., Mugnai, A. and Levizzani, V., 2000, Combining SSM/I, TRMM and infrared geostationary satellite data in a near-real time fashion for rapid precipitation updates: advantages and limitations. In *Proceedings of the 2000 EUMETSAT Meteorological Satellite Data Users' Conference*, Bologna, Italy, 29 May–2 June 2000, pp. 705–707.

Wei, C., 2003, Study on rainfall estimation using weather satellite imagery. PhD thesis, University of Taiwan, Taiwan.

Xu, L., Gao, X., Sorooshian, S., Arkin, P.A. and Imam, B., 1999, A microwave infrared threshold technique to improve the GOES precipitation index. *Journal of Applied Meteorology*, **38**, pp. 569–579.